Magnetic field induced tunneling and relaxation between orthogonal configurations in solids and molecular systems

N. S. Averkiev,[1,*] I. B. Bersuker,[2] V. V. Gudkov,[3] I. V. Zhevstovskikh,[4,3] K. A. Baryshnikov,[1] M. N. Sarychev,[3] S. Zherlitsyn,[5] S. Yasin,[5,†] and Yu. V. Korostelin[6]

[1]*Ioffe Institute, St. Petersburg 194021, Russia*

[2]*Institute for Theoretical Chemistry, the University of Texas at Austin, Austin, Texas 78712, USA*

[3]*Ural Federal University, Ekaterinburg 620002, Russia*

[4]*M. N. Miheev Institute of Metal Physics of Ural Branch of RAS, Ekaterinburg 620137, Russia*

[5]*Hochfeld-Magnetlabor Dresden (HLD-EMFL), Helmholtz-Zentrum Dresden-Rossendorf, Dresden D-01314, Germany*

[6]*P. N. Lebedev Physical Institute RAS, Moscow 119991, Russia*

(Received 23 February 2017; published 25 September 2017)

We report the effect of magnetic field induced quantum tunneling and relaxation transitions between orthogonal configurations in polyatomic systems where no tunneling is expected. Typical situations of this kind occur in molecular systems and local centers in crystals in ground and excited electronic T states, subject to the $T\otimes e$ problem of the Jahn-Teller effect, where the wave functions of the three tetragonally distorted configurations are orthogonal. A detailed microscopic theory of this effect shows how the magnetic field violates the orthogonality between the latter allowing for tunneling and relaxations, which decrease in strong fields due to the induced decoherence. The novel effect is demonstrated experimentally as a big, sharp peak in ultrasound attenuation by Cr^{2+} centers in ZnSe:Cr^{2+} in the magnetic field $B = 0.15$ T at the temperature below 8 K. It may influence a variety of magnetic, electronic, and photonic properties of any system in an electronic T state.

DOI: 10.1103/PhysRevB.96.094431

I. INTRODUCTION

There is well-known influence of magnetic fields on tunneling effects, e.g., in magnetoresistance and in magnetic tunnel junctions [1,2], resonance tunneling in high-spin molecules [3], and tunneling induced by phonons in magnetic molecules [4]. Distinguished from these works, we discovered magnetic field induced tunneling between local configurations in polyatomic systems with orthogonal electronic states, for which no tunneling is expected, the tunneling levels being produced by the magnetic field. The unlimited number of such systems includes any high-symmetry polyatomic group (impurity and vacancy centers in cubic crystals and similar molecular systems with cubic and icosahedral symmetry in different aggregate states, including thin films and quantum dots) in a threefold degenerate ground or excited electronic T state subject to the $T\otimes e$ problem of the Jahn-Teller (JT) effect (JTE) [5–7] (in slightly distorted cubic symmetry the results below should be modified following the transformation of the JTE into the pseudo-JTE [8]). With nonzero spin in these states the spin-orbital interaction is usually much smaller than the vibronic coupling that produces the JTE, at least for $3d$ transition-metal centers, hence it can be considered as a perturbation to the JTE, its influence being strongly reduced by the so-called vibronic reduction factors [6]. In these cases, the adiabatic potential energy surface (APES) has three equivalent minima along the three tetragonal distortions (distortions caused by e-type local displacements of atoms [6] distinguishing C_4 axes in octahedral and C_2 axes in tetrahedral atomic configurations, or distinguishing axes of a cubic crystal), but the three electronic functions of the distorted configurations in the minima are orthogonal, so no tunneling or direct relaxation transitions between them are allowed. This is the only multiminimum JTE problem where tunneling between the equivalent minima in the ground state is forbidden [6].

In this paper we show that an external magnetic field removes this prohibition, producing a new channel of tunneling and direct relaxation transitions between the distorted orthogonal configurations. We demonstrate both the theory and ultrasonic experimental observations of the novel effect using the Cr^{2+} impurities in the crystal ZnSe:Cr^{2+} as a typical example. This choice is motivated by the fact that the type of tunneling and relaxation under consideration involves nuclear displacements that can be tested by means of ultrasonic experiments (for which the crystal state is the best study *terrene*), and the study of the JTE in impurity crystals by means of ultrasound proved to be most efficient [9–12]. In the impurity center Cr^{2+} in the ZnSe crystal the ground electronic state is electronically threefold degenerate with three orbital wave functions of a hole in the closed-shell $3d^5$ configuration [10,13,14], transforming as vectors. They can be described by an orbital momentum operator with $L = 1$, hence being subjects to magnetic field influence. Experimental data [10,13,14] show that the JTE distortions in the impurity center under consideration are tetragonal, thus evidencing to the $T\otimes e$ problem.

Tunneling effects in JT systems were predicted in 1962 [15] and observed in optical, ESR, and ultrasonic experiments in a variety of systems (see, e.g., in Refs. [6,9,16,17]). In ultrasonic experiments tunneling manifests itself in the temperature dependence of relaxation time $\tau_{\rm rel}$, where by lowering the temperature the function $\tau_{\rm rel}(1/T)$ changes from $\tau_{\rm rel} \approx \nu_0^{-1} \exp(V_0/k_BT)$ in the activation mechanism (V_0 is the activation energy and k_B is the Boltzmann constant) to the tunneling mechanism with vanishing temperature

*averkiev.les@mail.ioffe.ru

†Present address: American University of the Middle East, College of Engineering and Technology, Egaila 54200, Kuwait.

dependence (see, e.g., Ref. [18]). The analysis of the temperature dependence of the relaxation time in zero magnetic field shows the absence of tunneling in the JT system of Cr^{2+} centers in ZnSe crystal. When a weak magnetic field is applied to the system at low temperatures, a sharp increase in the attenuation of ultrasound is observed. A microscopic theory is developed showing that the magnetic field produces a new relaxation channel associated with tunneling between the orthogonal distorted configurations, made possible due to magnetic-induced coupling between their orbital states.

II. EXPERIMENT

A high-quality ZnSe single crystal doped with Cr atoms was grown by a technology reported in Ref. [19]. The concentration of the chromium impurities, $n_{Cr} = 3.8\times10^{18}$ cm^{-3}, was determined from the absorption spectrum of the crystal. The sample had the form of a parallelepiped with a distance between the parallel faces of 4.7 mm. Experiments were carried out at the Dresden High Magnetic Field Laboratory using a phase-sensitive detection technique [20]. Ultrasonic waves were generated and detected by $LiNbO_3$ thin-film transducers, which were attached to the polished faces of the sample. The frequencies of the transverse ultrasonic modes were (in MHz) 33 (fundamental frequency), 119, 282, 360, and 449 (the third, ninth, eleventh, and fifteenth harmonics, respectively). The shear ultrasonic waves are induced to propagate along the crystallographic axis [110] with the polarization along $[1\bar{1}0]$. The attenuation coefficient of this slow shear wave is determined by the imaginary parts of the elastic modulus $C_s = (C_{11} - C_{12})/2$, $\alpha = (\omega/2v_s)(\mathrm{Im}\{C_s\}/\mathrm{Re}\{C_{s0}\})$, where $v_s = \sqrt{C_s/\varrho}$, ϱ denotes the mass density of the crystal, $C_{s0} = C_s(B = 0)$, and ω is the cyclic frequency of the ultrasound. The measurements in static magnetic fields were carried out by using a superconducting magnet.

In our preliminary study the attenuation peak was observed for only the slow shear wave in relatively weak magnetic fields (at about 0.1 T) at the temperature 2 K and for only one frequency of the ultrasound $\omega/2\pi = 24$ MHz [21] (the vector of magnetic induction **B** was parallel to the [110] axis). Based on this restricted information it was preliminarily assumed that the peak is of resonance origin. To understand better the nature of the attenuation peak we carried out a more detailed investigation using a wider interval of ultrasound frequencies (33–449 MHz), the magnetic field dependence of the attenuation was measured at several fixed temperatures below 20 K, and the temperature dependence of attenuation was measured at fixed magnetic fields, starting at 1.3 K. In addition, the experiments have been carried out with other direction of the magnetic field with respect to the direction of the wave propagation, namely, for **B** parallel to [001] and $[1\bar{1}0]$ crystallographic axes, respectively. The results of the experiments are shown in Figs. 1–3.

Following Fig. 1, we see that weak magnetic fields increase significantly the attenuation of the slow shear wave of the ultrasound, reaching a maximum at $B \approx 0.15$ T. Further increase of the field induction decreases the attenuation. The peak degrades with temperature and disappears at $T >$ 9 K. For $\mathbf{B} \parallel [1\bar{1}0]$ the peak of attenuation is quite similar to the peak for $\mathbf{B} \parallel [110]$, while for $\mathbf{B} \parallel [001]$ the attenuation

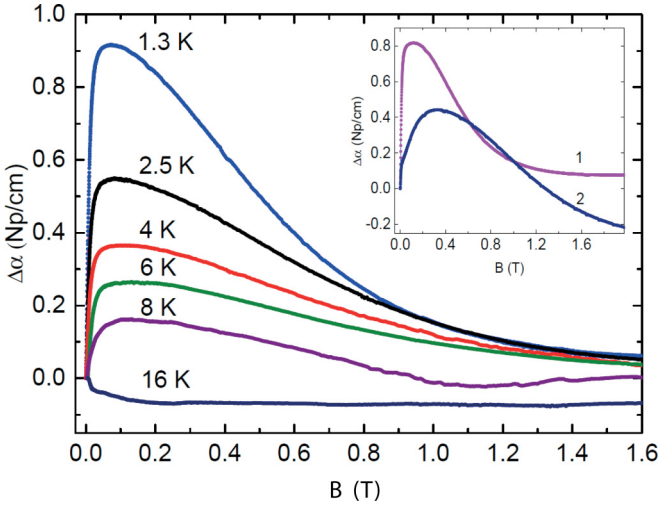

FIG. 1. Magnetic field dependence of ultrasound attenuation $\Delta\alpha = \alpha(B) - \alpha(0)$ at different temperatures, at the frequency $\omega/2\pi = 33$ MHz and magnetic induction $\mathbf{B} \parallel [110]$. Inset: the peak of attenuation in magnetic fields at $T = 1.3$ K at the same frequency but different directions of **B**: curve 1 — $\mathbf{B} \parallel [1\bar{1}0]$, curve 2 — $\mathbf{B} \parallel [001]$.

is different (see the inset in Fig. 1). However, in all these cases there is a peak of ultrasonic attenuation below 1 T. The data obtained at various frequencies (Fig. 2) show that the position of the attenuation peak along the B scale does not depend significantly on the ultrasound frequency. This contradicts the previous assumption about the resonant nature of the attenuation peak. Moreover, the temperature dependence of attenuation measured at various magnetic fields (Fig. 3) revealed a sharp increase of attenuation below 4 K when the magnetic field is applied, and the growth of attenuation is slowing and decreasing with increasing magnetic fields B. Obviously, anomalies of ultrasound attenuation detected at low temperatures and weak magnetic fields have a common origin.

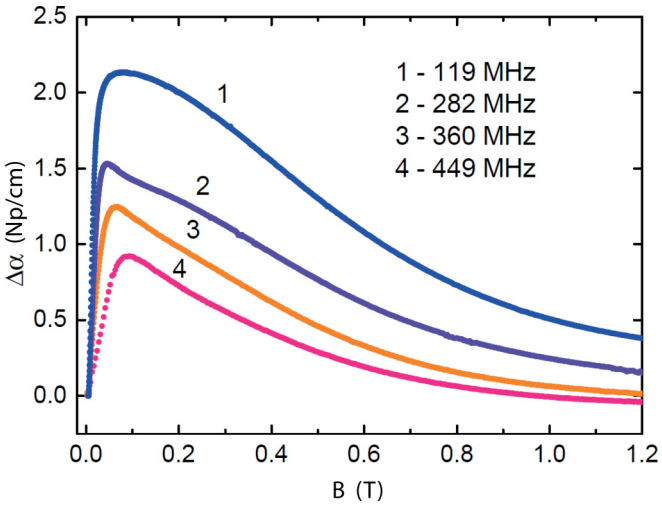

FIG. 2. Magnetic field dependence of ultrasound attenuation $\Delta\alpha = \alpha(B) - \alpha(0)$ at $T = 1.3$ K, $\mathbf{B} \parallel [110]$, and different frequencies (in MHz): 119, 282, 360, and 449 for curves 1, 2, 3, and 4, respectively.

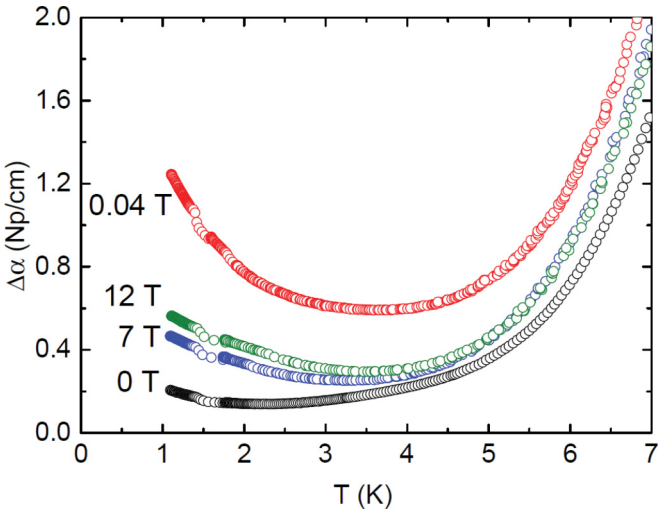

FIG. 3. Temperature dependence of ultrasound attenuation $\Delta\alpha = \alpha(T) - \alpha(T_0)$ for $T_0 = 30$ K, frequency $\omega/2\pi = 33$ MHz, and several indicated magnetic fields $\mathbf{B} \parallel [110]$.

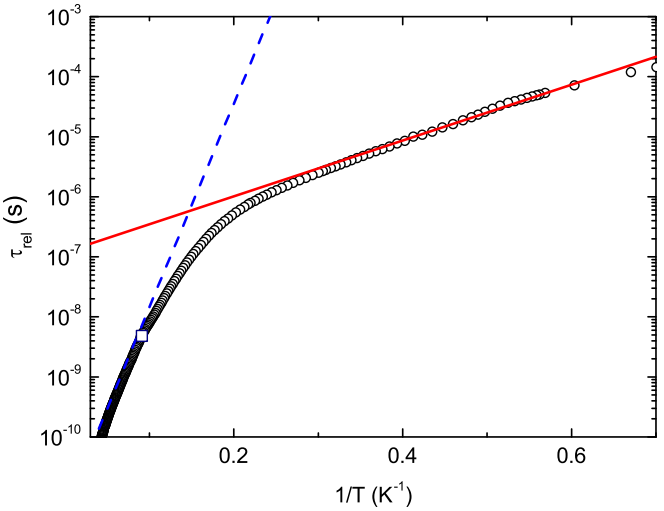

FIG. 4. Relaxation time versus $1/T$ obtained at the ultrasound frequency $\omega/2\pi = 33$ MHz (circles) in zero magnetic field. The white square corresponds to $\omega\tau_{\rm rel} = 1$ indicating the separation of the regime $\omega\tau_{\rm rel} > 1$ (low temperatures) from $\omega\tau_{\rm rel} < 1$ (high temperatures). Red solid and blue dashed lines can be attributed to one-phonon activation processes with activation energies $V_0^{(1)} = 0.9$ meV and $V_0^{(2)} = 6.7$ meV, respectively. The activation process with $V_0^{(1)} = 0.9$ meV with no saturation means there is no tunneling in zero magnetic fields.

The relaxation origin of ultrasonic attenuation in the ZnSe:Cr^{2+} crystal was revealed in the investigation of the temperature dependence of attenuation $\alpha(T)$ in zero magnetic field [10]. The peak of attenuation at about 11 K was interpreted as due to the relaxation between the three equivalent minima of the APES distorted by the propagating ultrasonic wave [10]. Further investigation of the function $\alpha(T)$ in fixed magnetic fields (up to 14 T) revealed significant influence of the latter on the position and shape of the temperature peak of the relaxation attenuation [22]. This means that the magnetic field dependence of ultrasound attenuation shown in Figs. 1 and 2 is of relaxation origin, at least at relatively weak fields.

To analyze the experimental results we extracted the temperature dependence of the relaxation time $\tau_{\rm rel}$ from the data of $\alpha(T)$ in zero magnetic field. The procedure to do this is described in Ref. [9] based on the assumption that the peak in $\alpha(T)$ is caused mainly by the relaxation in the system of noninteracting JT centers. The contribution to the ultrasound attenuation by other mechanisms, the background attenuation $\alpha_b(T)$ at low temperatures, is approximated by a smooth function [$\alpha_b(T) = -0.712 + 0.048T^{0.4} + 0.67/(3.2T - 0.17)^{0.4} - 0.0015T$ while the attenuation $\alpha(T)$ is measured from the level of $\alpha(T = 30\ {\rm K})$]. Then the relaxation attenuation by the JT centers $\alpha_{\rm rel}(T) = \alpha(T) - \alpha_b(T)$, and [9]

$$\tau_{\rm rel} = \frac{1}{\omega}\left[\frac{\alpha_{\rm rel}(T_1)T_1}{\alpha_{\rm rel}(T)T} \pm \sqrt{\left(\frac{\alpha_{\rm rel}(T_1)T_1}{\alpha_{\rm rel}(T)T}\right)^2 - 1}\right], \qquad (1)$$

where T_1 is the temperature at $\omega\tau_{\rm rel} = 1$, which can be determined from the position of the maximum of the function $f(T) = \alpha_{\rm rel}(T)T$. The physically correct solutions are provided by the sign "+" before the square root for $T < T_1$, and sign "−" for $T > T_1$. Figure 4 shows $\tau_{\rm rel}$ versus $1/T$ in a semilogarithmic scale for the system of Cr^{2+} centers in ZnSe in zero magnetic field. Note that the relaxation time here equals $\approx 10^{-6}$ s at 4.2 K, which is much higher than the typical values for the JT centers in other crystals, 10^{-9}–10^{-7} s at 4.2 K [11,12,17,23–26]. In our case, such a slow relaxation at low temperatures may serve as indirect evidence of the absence of tunneling transitions. The red solid line and blue dashed line in Fig. 4 indicate two activation regimes for $\tau_{\rm rel} \propto \exp(V_0^{(k)}/k_BT)$ with $k = 1$ (low-temperature regime) and $k = 2$ (high-temperature regime), respectively. In Fig. 4 the activation mechanism dominates at high temperatures changing the regime below ≈6 K, but no saturation occurs in this temperature range. Hence, there is no tunneling in ZnSe:Cr^{2+} in zero magnetic field. The slope of $\tau_{\rm rel}(1/T)$ at low temperatures yields the activation energy of 0.9 meV, which is in a good agreement with the theoretical model derived from EPR studies [14] (see below).

III. THEORY

A. Jahn-Teller center

As mentioned above, the impurity center of the Zn-substitutional ion Cr^{2+} in the ZnSe crystal forms the impurity complex $Cr_{Zn}4Se$ subject to JTE with the $T\otimes e$ problem [10,13,14]. In this case, the APES in the space of the two normal e-type atomic displacements of the JT complex, Q_2 and Q_3, consists of three independent parabolic surfaces intersecting in the point of the threefold degeneracy [6] as it is shown in Fig. 5. The minima of these paraboloids correspond to three equivalent tetragonal distortions of the tetrahedral impurity surroundings along, respectively, the x, y, and z axes of the crystal. The vibronic states in the minima are described by three wave functions $\phi_x|x\rangle$, $\phi_y|y\rangle$, $\phi_z|z\rangle$, where $|x\rangle$, $|y\rangle$, $|z\rangle$ are the three orbital electronic T_2 states, and $\phi_j = \phi_j(Q_2 - Q_2^{(j)}, Q_3 - Q_3^{(j)})$, $j = x,y,z$, are the vibrational wave functions of linear oscillators localized near the minima points

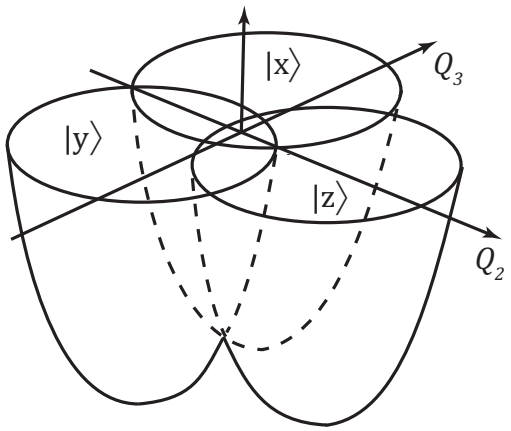

FIG. 5. Three independent potential energy paraboloids for the atomic oscillations in the case of the $T\otimes e$ problem of the JTE [6]. Each electronic orbital wave function $|x\rangle, |y\rangle, |z\rangle$ describes an independent configuration of the Cr^{2+} environment, tetragonally distorted along the x, y, and z axes, respectively, with corresponding three oscillator functions ϕ_x, ϕ_y, ϕ_z in the minima of the paraboloids.

$(Q_2^{(j)}, Q_3^{(j)})$, respectively. EPR study [14] shows that the ground state has a fivefold spin degeneracy, subject to the $S = 2$ total spin. The $T\otimes e$ problem still holds as the vibronic interaction is much stronger than the spin-orbit coupling. However, the spin-orbit interaction is important in determining the ground state of the system in weak magnetic fields.

The complete set of eigenstates of the center corresponds to a fifteenfold degeneracy and is described by the direct product of a threefold degenerate vibronic state by a fivefold degenerate spin state corresponding to a total spin $S = 2$. The spin degeneracy is removed by a weak spin-orbit interaction [13,14]. The spin-orbit Hamiltonian consists of linear $(\hat{\mathbf{L}}\cdot\hat{\mathbf{S}})$ terms and corresponding quadratic terms of $(\hat{\mathbf{L}}\cdot\hat{\mathbf{S}})^2$ (stemming, for instance, from the spin-spin interaction [13,14,27]), which also couple spin and orbital states of the center. There are no $(\hat{\mathbf{L}}\cdot\hat{\mathbf{S}})$ terms of higher orders because for $L = 1$ operators L_j^3 are determined by linear combinations of L_j^2 and L_j. The total Hamiltonian of the spin-orbit coupling takes the form:

$$\hat{H}_{SO} = \lambda_0(\hat{\mathbf{L}}\cdot\hat{\mathbf{S}}) - \lambda_1(\hat{L}_\theta\hat{S}_\theta + \hat{L}_\varepsilon\hat{S}_\varepsilon) - \lambda_2(\hat{L}_\xi\hat{S}_\xi + \hat{L}_\eta\hat{S}_\eta + \hat{L}_\zeta\hat{S}_\zeta). \quad (2)$$

Here λ_0 is the main spin-orbit coupling constant, while λ_1 and λ_2 are the constants of quadratic spin-orbit coupling terms, which are independent due to the cubic symmetry of the crystal. Similarly to the notation in Ref. [14], $\hat{L}_\theta$ and $\hat{L}_\varepsilon$ and $\hat{L}_\xi$, $\hat{L}_\eta$, and $\hat{L}_\zeta$ are quadratic combinations of $\hat{L}_x, \hat{L}_y, \hat{L}_z$ components of the operator of the orbital momentum $\hat{\mathbf{L}}$ (with the quantum number $L = 1$) that transform, respectively, as the E and T_2 irreducible representations of the T_d symmetry group. The same transformations are assumed for the spin operators $\hat{S}_\theta$, $\hat{S}_\varepsilon$ and $\hat{S}_\xi$, $\hat{S}_\eta$, $\hat{S}_\zeta$ quadratic in components of spin $\hat{\mathbf{S}}$ with $S = 2$.

Besides the spin-orbit interaction, the degeneracy of eigenstates can be reduced by magnetic fields. The interaction with magnetic fields reads as

$$\hat{H}_B = g_S\mu_B(\mathbf{B}\cdot\hat{\mathbf{S}}) + g\mu_B(\mathbf{B}\cdot\hat{\mathbf{L}}), \quad (3)$$

where $g = 1$ is the orbital g factor (the Cr^{2+} ion has four electrons with parallel spins in the $3d$ shell and its orbital behavior is described by a hole), $g_S = 2$ is the spin g factor, and μ_B is the Bohr magneton. Assuming that the Hamiltonians (2) and (3) are perturbations to the basic fifteenfold degenerate ground state of the JT complex, we obtain for the total Hamiltonian of the system the following block-matrix expression of the second order of perturbation theory (see, e.g. Ref. [28]):

$$\hat{H} = \begin{pmatrix} g_S\mu_B(\mathbf{B}\cdot\hat{\mathbf{S}}) + D\hat{S}_x^2 & -ig\mu_B B_z\epsilon & ig\mu_B B_y\epsilon \\ ig\mu_B B_z\epsilon & g_S\mu_B(\mathbf{B}\cdot\hat{\mathbf{S}}) + D\hat{S}_y^2 & -ig\mu_B B_x\epsilon \\ -ig\mu_B B_y\epsilon & ig\mu_B B_x\epsilon & g_S\mu_B(\mathbf{B}\cdot\hat{\mathbf{S}}) + D\hat{S}_z^2 \end{pmatrix}, \quad (4)$$

where

$$D = \frac{\lambda_0^2}{3E_{JT}} - \frac{\lambda_1}{2} - \frac{20\lambda_2^2}{27E_{JT}},$$
$$\epsilon = \langle\phi_j|\phi_{k\neq j}\rangle = \exp(-3E_{JT}/2\hbar\omega_e). \quad (5)$$

Here ϵ is the vibronic reduction factor emerging from the overlap of vibrational ϕ functions of different distorted configurations [6,28]. E_{JT} is the Jahn-Teller stabilization energy, ω_e is the ground-state frequency of e vibrations in the minima configurations; the value of the parameter $D = -0.31$ meV is known directly from the EPR measurements for Cr^{2+} in ZnSe [14].

In Eq. (4) we neglected the spin-orbit terms in the off-diagonal positions. Such terms, if significant, would lead to peculiarities that are more visible in the temperature dependence of ultrasound attenuation at very low temperatures in zero magnetic field. The small increase of attenuation below 1.5 K in zero magnetic field (see Fig. 3), which could stem from these spin-orbit terms, as well as from other random local deformations in the crystal, can be neglected compared with the strong increase of attenuation in the whole temperature interval at $B = 0.04$ T, discussed below. In addition, we neglect the contribution of higher than second-order terms in spin operators, which were shown to be weak in the case of Cr^{2+} in ZnSe [14]. The matrix elements in Eq. (4) are themselves matrices of dimension 5×5 corresponding to the spin degrees of freedom of the center. Still, the rows and columns of the 3×3 matrix in Eq. (4) number the three orbital states of the center from left to right and from top to bottom, respectively.

B. Interaction with ultrasound

The interaction $\hat{V}$ of the slow shear ultrasonic wave propagating along the [110] direction in the crystal with the chromium center, in the basis of the wave functions

$\phi_x|x\rangle, \phi_y|y\rangle, \phi_z|z\rangle$, is:

$$\hat{V} = \begin{pmatrix} b\sin\omega t & 0 & 0 \\ 0 & -b\sin\omega t & 0 \\ 0 & 0 & 0 \end{pmatrix}, \tag{6}$$

where ω is a frequency of ultrasound wave, $b = ku_0 b_T/\sqrt{2}$, k is the amplitude of the wave vector, $u_0/\sqrt{2}$ is the amplitude of the elastic deformation of the crystal caused by the sound, and b_T is the deformation constant in the Bir-Pikus Hamiltonian of electron-deformation interactions [29].

The coefficient of ultrasonic wave attenuation (by amplitude) in the approximation of small attenuation, the sound wave remaining monochromatic, is defined as

$$\alpha = \frac{1}{2}\frac{n_{Cr}P}{\varepsilon \cdot v}, \tag{7}$$

where $\varepsilon \cdot v$ is the sound-wave energy flux density, $\varepsilon = \varrho\omega^2 u_0^2$ is the energy density of the ultrasonic wave that propagates along [110] with the polarization along [1$\bar{1}$0] at frequency ω, v is the phase velocity of the wave, n_{Cr} is the concentration of Cr^{2+} centers, and P is the average power of the wave absorbed by the center,

$$P = -\overline{\mathrm{Tr}(\hat{\rho}\dot{\hat{V}})}. \tag{8}$$

Here $\dot{\hat{V}}$ is the time derivative of the operator $\hat{V}$ of Eq. (6), $\hat{\rho}$ is the operator of the density matrix of the center, and Tr denotes the operation of taking the trace of the matrix.

C. Zero magnetic field

The ground state of the Cr^{2+} center in the ZnSe crystal in zero magnetic field is sixfold degenerate and consists of three orbital wave functions multiplied by the proper doubly degenerate spin state $|S_j^2 = 4\rangle$, corresponding to a given well of the adiabatic potential $j = x,y,z$. We introduce the notation $|S_z = 2\rangle = |\alpha\rangle$, $|S_z = 1\rangle = |\beta\rangle$, $|S_z = 0\rangle = |\gamma\rangle$, $|S_z = -1\rangle = |\bar{\beta}\rangle$, $|S_z = -2\rangle = |\bar{\alpha}\rangle$. When the magnetic field is applied along the [110] direction, the sixfold degeneracy is removed and the wave functions of the eigenstates corresponding to the energy $E = -\sqrt{2}g_S\mu_B B$ (read off from the energy of the ground state in the zero field) have the form $|1\rangle = \phi_x|x\rangle(-|\alpha\rangle + 2|\beta\rangle - \sqrt{6}|\gamma\rangle + 2|\bar{\beta}\rangle - |\bar{\alpha}\rangle)/4$, $|2\rangle = \phi_y|y\rangle(-|\alpha\rangle - 2i|\beta\rangle + \sqrt{6}|\gamma\rangle + 2i|\bar{\beta}\rangle - |\bar{\alpha}\rangle)/4$; wave functions corresponding to the energy $E = 0$ have the form $|3\rangle = \phi_z|z\rangle|\alpha\rangle$ and $|4\rangle = \phi_z|z\rangle|\bar{\alpha}\rangle$; finally, excited states corresponding to $E = \sqrt{2}g_S\mu_B B$ are read as $|5\rangle = \phi_y|y\rangle(-|\alpha\rangle + 2i|\beta\rangle + \sqrt{6}|\gamma\rangle - 2i|\bar{\beta}\rangle - |\bar{\alpha}\rangle)/4$ and $|6\rangle = \phi_x|x\rangle(|\alpha\rangle + 2|\beta\rangle + \sqrt{6}|\gamma\rangle + 2|\bar{\beta}\rangle + |\bar{\alpha}\rangle)/4$. If we assume that $B = 0$, the ground eigenstates are: $|1\rangle,|2\rangle,|3\rangle,|4\rangle,|5\rangle,|6\rangle$.

The nearest excited state is split off by spin-orbit interaction in energy upwards by $|3D| \approx 0.9$ meV [14], and it is also sixfold degenerate, but its spin states already meet the condition $S_j^2 = 1$: $|7\rangle = \phi_x|x\rangle(|\alpha\rangle - |\beta\rangle + |\bar{\beta}\rangle - |\bar{\alpha}\rangle)/2$, $|8\rangle = \phi_y|y\rangle(-|\alpha\rangle - i|\beta\rangle - i|\bar{\beta}\rangle + |\bar{\alpha}\rangle)/2$, $|9\rangle = \phi_z|z\rangle|\beta\rangle$, $|10\rangle = \phi_z|z\rangle|\bar{\beta}\rangle$, $|11\rangle = \phi_y|y\rangle(-|\alpha\rangle + i|\beta\rangle + i|\bar{\beta}\rangle + |\bar{\alpha}\rangle)/2$, $|12\rangle = \phi_x|x\rangle(-|\alpha\rangle - |\beta\rangle + |\bar{\beta}\rangle + |\bar{\alpha}\rangle)/2$. The last excited state, split off by $|4D|$, is threefold degenerate, as each orbital state is accompanied by the corresponding spin state $|S_j^2 = 0\rangle$: $|13\rangle = \phi_x|x\rangle(\sqrt{3}|\alpha\rangle - \sqrt{2}|\gamma\rangle + \sqrt{3}|\bar{\alpha}\rangle)/\sqrt{8}$, $|14\rangle = \phi_y|y\rangle(\sqrt{3}|\alpha\rangle + \sqrt{2}|\gamma\rangle + \sqrt{3}|\bar{\alpha}\rangle)/\sqrt{8}$, $|15\rangle = \phi_z|z\rangle|\gamma\rangle$.

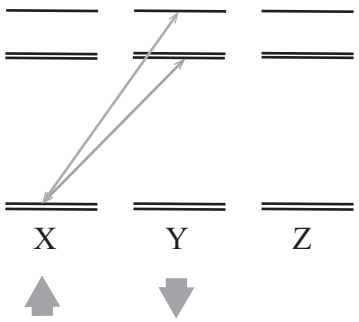

FIG. 6. The scheme of the energy levels of the $Cr_{Zn}4Se$ complex in zero magnetic field with X,Y,Z unfolding toward the three potential wells corresponding to the orbital states $|x\rangle$, $|y\rangle$, $|z\rangle$ of the Cr^{2+} center. The levels are split by the spin-orbit interaction. Thick gray arrows show the direction of the energy level shift due to the slow shear ultrasonic wave propagating along the [110] direction. Thin gray arrows show two main admissible one-phonon transitions.

As mentioned above, an important feature of the $T\otimes e$ problem in zero magnetic field is the absence of tunneling between the ground states of the three configurations of the three minima of the APES (Fig. 5) because of the orthogonality of their orbital wave functions. Accordingly, relaxation due to tunneling transitions between them is also forbidden, hence the observed relaxation at low temperatures is caused by other processes. Let us evaluate the intensity W of direct one-photon transitions in the system shown schematically in Fig. 6. Calculated according to the golden rule of quantum mechanics, and by averaging over the phonon density of states, we get [27]:

$$W = \frac{2\pi}{\hbar^2}G(\Delta E)|M(\Delta E)|^2\left(N_{ph}(\Delta E) + \frac{1\pm 1}{2}\right), \tag{9}$$

where "+" is related to phonon emission process and "−" to phonon absorption process, $N_{ph}(\Delta E)$ is the number of phonons in equilibrium at the given energy and temperature, $G(\Delta E)$ is the density of states of acoustic phonons with the energy ΔE,

$$G(\Delta E) = \frac{3\Sigma}{2\pi^2\hbar^2 v^3}(\Delta E)^2, \tag{10}$$

and $M(\Delta E)$ is the matrix element of the interaction of the center with a phonon with the energy ΔE

$$|M(\Delta E)|^2 = \delta\frac{3d_T^2}{2\Sigma\varrho v^2}\Delta E. \tag{11}$$

Here the parameter δ emerges as a result of averaging over all directions of the phonons taking into account the selection rules and the overlapping wave functions of the center (the estimate is $\delta \approx \epsilon^2/24$), Σ is the volume of the sample crystal, and d_T is the constant of the deformation potential responsible for the overlap of the orbital states $|x\rangle$, $|y\rangle$, $|z\rangle$ by the phonon displacements.

Since the temperature range of interest follows the condition $k_B T \ll |3D|$, the relaxation is determined only by the

processes of transitions from the ground state to the nearest excited state, and only the most inertial excitation processes (related to absorption of phonons) with $\tau_{\rm rel}^{-1} \propto N_{\rm ph} \propto \exp(-|3D|/k_BT)$ contribute significantly to the relaxation time in Eq. (9), the spontaneous emission being very fast. Consequently, the slope of the temperature dependence of the relaxation time is strictly determined by the quantity $|3D|$. The following parameters of the ZnSe crystal were used in the calculation: $\varrho = 5.27$ g/cm^3, $v = 1.8\times10^5$ cm/s. In accordance with further calculations below for nonzero magnetic fields we take $E_{\rm JT}/\hbar\omega_e = 1.2$, which corresponds to the overlap of the vibrational wave functions [Eq. (5)] $\epsilon \approx 0.17$. This reflects a relatively weak to moderate JTE in the $Cr_{Zn}4Se$ impurity complex (there are no well-established evaluations for $E_{\rm JT}$ and ω_e in the literature, but many estimates for impurity centers yield for their ratio approximate values within 1 and 5 [13,30–32]). Then from Eq. (9), in comparison with the experimental values of relaxation times [33] we get for the value of the lattice deformation constant $d_{\rm T} \approx 10$ meV, which seems to be reasonable, albeit relatively small for semiconductors [34,35]. The smaller the ϵ values the greater the estimated $d_{\rm T}$ magnitude. Note, however, that the value of $d_{\rm T}$ has no effect on the slope of the temperature dependence $\tau_{\rm rel}(1/T)$.

D. Nonzero magnetic fields

When a magnetic field is applied to the sample in the direction [110] the orbital splitting is not very significant in forming the energy spectrum of the center mostly due to the vibronic reduction factor in Eq. (4). Because of the vibronic reduction, the shifts of the vibronic energy levels in low magnetic fields are very small. If they are less than the natural broadening of the energy levels (meaning small decoherence time τ_2, see below), the break of the orthogonality due to orbital coupling in magnetic fields produces an additional channel of relaxation transitions between the APES minima, increasing the relaxation rate, and hence the ultrasound attenuation. In stronger fields the off-diagonal contribution to the energy levels in different wells makes them nonequivalent, degrading the relaxation attenuation of the sound, and this explains the decrease of attenuation (see the next section).

Neglecting the off-diagonal terms in Eq. (4) originated from the orbital part of the interaction with the magnetic field, we obtain a block-diagonal form of the Hamiltonian. In this approximation, the splittings of the energy levels of the spin states in each potential well X,Y,Z, by the magnetic field are independent from each other. When $\mathbf{B} \parallel [110]$ the X and Y states in Fig. 6 are split, while the degeneracy of Z states is conserved in weak fields.

In nonzero magnetic fields the changes in the probabilities of one-phonon transitions, shown in Fig. 6 and described by Eq. (9), as well as the changes in the population of the energy levels [36], do not explain the observed sharp peak of ultrasound attenuation in weak magnetic fields (Figs. 1 and 2). Indeed, in the temperature range from 1–4 K, the rate of one-phonon processes and the population of the energy levels in fields below 1 T do not change significantly. At $B \approx 1$ T the splitting of the energy levels becomes comparable with k_BT, but the sharp increase in ultrasonic absorption is observed at $B \approx 0.1$ T. As mentioned above, we explain the observed sharp peak of relaxation attenuation in weak fields as due to the magnetic field induced tunneling transitions between the orthogonal X,Y, and Z configurations of the center. The additional relaxation channel between the distorted configurations is opened due to the coupling between their orbital wave functions by the magnetic field, while the overlap between their vibrational wave functions is *a priori* nonzero [see Eq. (5)].

We are interested in relatively low temperatures ($T \ll |3D|/k_B$) and relatively weak fields ($B \ll |3D|/g_S\mu_B$), hence only six ground states from the full set of 15 states will make a contribution in formation of the new states in magnetic fields in this region of parameters. The Hamiltonian in the basis of the ground state $|6\rangle,|1\rangle,|5\rangle,|2\rangle,|3\rangle,|4\rangle$ (this sequence of wave functions reflects the numbering of spin-state pairs associated with the orbital functions $|x\rangle, |y\rangle, |z\rangle$, successively) taking into account the orbital coupling in the magnetic field and interaction of orbital states of the center with the slow shear ultrasonic wave [Eq. (6)] is as follows:

$$\hat{H} = \begin{pmatrix} \hbar\Delta U + b(t) & 0 & 0 & 0 & -i\hbar\Gamma/4 & -i\hbar\Gamma/4 \\ 0 & -\hbar\Delta U + b(t) & 0 & 0 & i\hbar\Gamma/4 & i\hbar\Gamma/4 \\ 0 & 0 & \hbar\Delta U - b(t) & 0 & -i\hbar\Gamma/4 & -i\hbar\Gamma/4 \\ 0 & 0 & 0 & -\hbar\Delta U - b(t) & -i\hbar\Gamma/4 & -i\hbar\Gamma/4 \\ i\hbar\Gamma/4 & -i\hbar\Gamma/4 & i\hbar\Gamma/4 & i\hbar\Gamma/4 & 0 & 0 \\ i\hbar\Gamma/4 & -i\hbar\Gamma/4 & i\hbar\Gamma/4 & i\hbar\Gamma/4 & 0 & 0 \end{pmatrix}, \tag{12}$$

Here $\Delta U = \sqrt{2}g_S\mu_B B/\hbar$ denotes the spin level splitting, $\Gamma = g\mu_B B\epsilon/\hbar$ denotes the effective tunneling parameter originated from the orbital coupling and vibrational functions overlap, and $b(t) = b\sin\omega t$ denotes the shift of the energy levels by the time-dependent action of the sound wave. Equation (12) shows that in the magnetic field $\mathbf{B} \parallel [110]$, two levels (associated with X and Y configurations) are shifted down in energy by $\hbar\Delta U$, two states (associated with the Z configuration) remain unaffected, and the remaining two states from X and Y configurations are shifted up by the same energy value $\hbar\Delta U$. Since ΔU is always much larger than Γ (because of the reduction factor ϵ) the magnetic field couples orbitally the states in X and Y configurations via the states in the Z configuration. In this situation the main results for

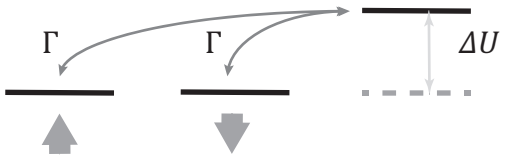

FIG. 7. The scheme of energy levels and tunneling transitions Γ (thin arrows) in the $Cr_{Zn}4Se$ complex for the direction of the magnetic field [110]. The thick arrows indicate a time-periodic splitting of the levels by the slow shear ultrasound wave propagating along the [110] direction. ΔU is the spin level splitting.

the relaxation attenuation of ultrasound by the Cr^{2+} center in ZnSe in a magnetic field $\mathbf{B} \parallel [110]$ can be obtained analytically from the generalization of the three-level scheme shown in Fig. 7.

Then we get for the Hamiltonian of the system in the three-level model illustrated in Fig. 7 the following expression:

$$\hat{H} = \begin{pmatrix} 0 & 0 & \hbar\Gamma/\sqrt{2} \\ 0 & 0 & \hbar\Gamma/\sqrt{2} \\ \hbar\Gamma/\sqrt{2} & \hbar\Gamma/\sqrt{2} & \hbar\Delta U \end{pmatrix}. \tag{13}$$

In this model, the interaction with a slow shear ultrasound wave is, as above, described by Eq. (6). Provided $b,\hbar\Gamma \ll \hbar\Delta U \ll k_BT$, where T is the temperature, the quasiequilibrium components of the density matrix are:

$$\rho_{11}^{(0)} = \frac{1}{3} + \frac{b\sin\omega t}{3k_BT}; \quad \rho_{22}^{(0)} = \frac{1}{3} - \frac{b\sin\omega t}{3k_BT};$$
$$\rho_{33}^{(0)} = \frac{1}{3} - \frac{\hbar\Delta U}{3k_BT}; \quad \rho_{12}^{(0)} = \rho_{21}^{(0)} = 0;$$
$$\rho_{13}^{(0)} = \rho_{31}^{(0)} = \rho_{23}^{(0)} = \rho_{32}^{(0)} = \frac{\hbar\Gamma}{3\sqrt{2}k_BT}. \tag{14}$$

With these density matrix elements the kinetic equations for the linear combinations of the nonequilibrium additives to the quasiequilibrium density matrix $z_1 = \rho_{22}^{(1)} - \rho_{11}^{(1)}$, $x_1 = \rho_{13}^{(1)} - \rho_{31}^{(1)} - \rho_{23}^{(1)} + \rho_{32}^{(1)}$, $x_3 = \rho_{13}^{(1)} + \rho_{31}^{(1)} - \rho_{23}^{(1)} - \rho_{32}^{(1)}$, and $y_1 = \rho_{12}^{(1)} - \rho_{21}^{(1)}$, in the linear in b approximation (i.e., $b \ll \hbar/\tau_2$) can be written as follows:

$$\begin{cases} \dot{z}_1 = -i\dfrac{\Gamma}{\sqrt{2}}x_1 - \tau_T^{-1}z_1 - \dfrac{2b\omega\cos\omega t}{3k_BT} \\ \dot{x}_1 = i\Delta U x_3 - i\sqrt{2}\Gamma z_1 - \dfrac{x_1}{\tau_2} \\ \dot{x}_3 = i\Delta U x_1 + i\sqrt{2}\Gamma y_1 - \dfrac{x_3}{\tau_2} \\ \dot{y}_1 = i\dfrac{\Gamma}{\sqrt{2}}x_3 - \dfrac{y_1}{\tau_2}. \end{cases} \tag{15}$$

Here τ_T is the temperature-dependent relaxation time in zero magnetic field, and τ_2 is the decoherence time. τ_T is described by one-phonon transitions via excited states [Eq. (9)]; changes in the rate of such one-phonon transitions in weak magnetic fields can be neglected, since we are exploring the region where $|g_S\mu_B B| \ll k_BT$. The decoherence time τ_2 is determined mainly by elastic processes, and therefore it does not contribute to the absorption of the sound power in zero field, but it plays a major role in relaxation due to the orbital coupling Γ that leads to the magnetic field induced tunneling. We assume that τ_2 is an additional parameter of the system, which remains almost unchanged in the range of magnetic fields and temperatures under consideration. Note that the difference between the relaxation time and the decoherence time, discussed here, is analogous to the difference between the times T_1 and T_2 in the theory of paramagnetic resonance [37].

The average power absorbed is $P = \overline{z_1 b\omega\cos\omega t}$ [see Eq. (8)]. We are looking for the steady solution for z_1 from the linear Eqs. (15). Then we get $P = b\omega\mathrm{Re}\{z\}$, where

$$z = \frac{\dfrac{b\omega\tau_2}{3k_BT}}{\dfrac{\tau_2}{\tau_T} + i\omega\tau_2 + \dfrac{\Gamma^2\tau_2^2}{1+i\omega\tau_2}\dfrac{1}{1+\dfrac{\Delta U^2\tau_2^2}{(1+i\omega\tau_2)^2+\Gamma^2\tau_2^2}}}. \tag{16}$$

At $\Gamma \ll 1/\tau_2$ this solution can be simplified by assuming that $\omega\tau_2 \ll 1$, $\omega \gg \tau_T^{-1}$, and $\Gamma^2\tau_2$:

$$z \approx \frac{b}{3k_BT\omega}\left(\tau_T^{-1} + \frac{\Gamma^2\tau_2}{1+\Delta U^2\tau_2^2}\right). \tag{17}$$

Then the coefficient of ultrasonic relaxation attenuation from Eq. (7) equals

$$\alpha = \frac{n_{\mathrm{Cr}}b_{\mathrm{T}}^2}{8\varrho v^3k_BT}\left(\rho_{11}^0 + \rho_{22}^0\right)\frac{1}{\tau}, \tag{18}$$

where $\rho_{11}^0 + \rho_{22}^0 = 2/3$ is the equilibrium population of the X and Y levels split by ultrasound (for $\hbar\Delta U \ll k_BT$), and we introduced an effective relaxation time that includes the tunneling in magnetic fields,

$$\frac{1}{\tau} = \tau_T^{-1} + \sum_{n,m}|\gamma_{nm}|^2\frac{2\Gamma^2\tau_2}{1+\Delta U_{nm}^2\tau_2^2}. \tag{19}$$

Here $\Delta U_{nm} = (E_n - E_m)/\hbar$ is the difference between the energy levels in different distorted configurations of $Cr_{Zn}4Se$ in the magnetic field (n and m run through all spin-orbital states in the different configurations), $\gamma_{nm} = \langle n|\mathbf{o}\cdot\hat{\mathbf{L}}|m\rangle$ is the off-diagonal matrix element of the Hamiltonian, which becomes nonzero in the magnetic field, $\mathbf{o} = \mathbf{B}/B$. In the simplified model of Fig. 7 $\gamma_{nm} = 1/\sqrt{2}$, but in reality this matrix element may be different. Equation (19) is valid for transitions from one configuration of $Cr_{Zn}4Se$ complex to another taking into account the overlap of all their 15 eigenstates induced by the magnetic field.

The second term in Eq. (19) stands for the rate of relaxation via the new channel opened by the magnetic field induced tunneling transitions. By magnitude, it can be comparable or larger than the rate of relaxation in zero field. This additional channel of relaxation leads to the increase in ultrasound attenuation, as demonstrated above, but it may affect also other optical, magnetic, and spin properties of crystals containing JT impurity or vacancy centers, subject to the $T\otimes e$ vibronic coupling problem.

IV. DISCUSSION

The results of calculations [33] using Eqs. (18) and (19) as well as experimental points are demonstrated in Fig. 8. The following parameter values are employed in these

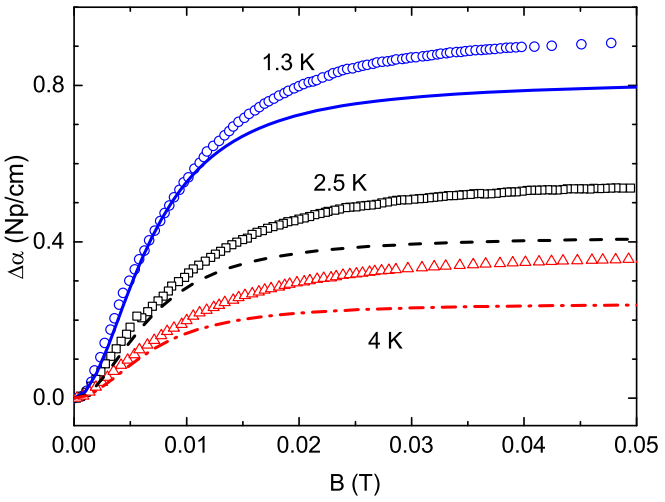

FIG. 8. Magnetic field dependence of attenuation of ultrasound of frequency $\omega/2\pi = 33$ MHz by Cr^{2+} centers in cubic ZnSe crystal at $T = 1.3$ K (blue circles), $T = 2.5$ K (black squares), and $T = 4$ K (red triangles) at $\mathbf{k} \parallel \mathbf{B} \parallel [110]$, $\mathbf{u_0} \parallel [1\bar{1}0]$, $\mathbf{k}$ is the wave vector and $\mathbf{u_0}$ is the polarization vector of the ultrasound wave. The solid line at $T = 1.3$ K, dash line at $T = 2.5$ K, and dash dot line at $T = 4$ K are the results of theoretical calculations carried out using Eqs. (18) and (19) with $\tau_2 = 6\times10^{-10}$ s and $E_{JT}/\hbar\omega_e = 1.2$. The field $B = 0.05$ T (the right edge of the figure) corresponds to the boundary of applicability of Eqs. (18) and (19), $\Gamma\tau_2 \approx 1/3$.

calculations: $n_{Cr} = 3.8\times10^{18}$ cm^{-3}, $b_T \approx 2$ eV (this estimate is obtained from ultrasound attenuation in zero magnetic field [10]), $\tau_2 = 6\times10^{-10}$ s and $E_{JT}/\hbar\omega_e = 1.2$. There are only two fitting parameters in calculations: the decoherence time τ_2 and the vibronic reduction factor that depends exponentially on the ratio $E_{JT}/\hbar\omega_e$. For τ_2, we assume that it is independent of the temperature and the magnetic field. The parameter $E_{JT}/\hbar\omega_e$, discussed at the end of Sec. III C, is not well known numerically. Our choice of $E_{JT}/\hbar\omega_e = 1.2$ is the result of fitting: with only these two parameters we fit all the three experimental curves in Fig. 8, thus showing that the theory explains the effect in the limits of its applicability. A closer fitting could be reached by simulating some dependence of τ_2 on temperature and magnetic field; this would increase the number of fitting parameters without significantly shedding light on the origin of the magnetic field induced tunneling.

Equation (19) is analogous to the expression for the relaxation time obtained by Vikhnin [38] for a somewhat similar statically deformed system of two potential wells with the static deformation modeled by the ΔU_{nm} term. We have generalized this result for relaxation time that contributes to the attenuation of a sound wave in a much more complicated system. In some aspects Eq. (19) is also analogous to the result for spin relaxation rates in the Dyakonov-Perel mechanism [39] if we set $\Delta U_{nm} = 0$. Note also that Eq. (19) allows for describing resonance tunneling between states with energy difference ΔU_{nm} if the tunneling element Γ is independent of ΔU_{nm}. However, in the case of magnetic field induced tunneling both Γ and ΔU_{nm} depend on the magnetic field, and the change in only ΔU_{nm} does not explain the decrease of attenuation in magnetic fields above 0.2 T, as well as the saturation at $\Gamma \propto \Delta U_{nm} \propto B$ (see Fig. 8). The decrease of attenuation in higher fields is caused by the transition to the quasiresonance mechanism of absorption instead of just relaxation (see below).

Equations (18) and (19) were derived under the condition of weak magnetic fields and $b, \hbar\Gamma \ll \hbar/\tau_2$, but the predecessor Eqs. (15) are valid also for b values for which the splitting of the $|x\rangle$ and $|y\rangle$ states by the ultrasound wave is much larger than that induced by the magnetic field, and the latter can be ignored as compared with the former. As no equilibrium population of the split levels is reached in the time of the wave period, the attenuation is relaxational, and the role of the magnetic field is to accelerate the relaxation via the newly opened tunneling channel. This takes place under the condition $b > \hbar\Gamma^2/\Delta U$ for $\mathbf{B} \parallel [110]$ or $\mathbf{B} \parallel [1\bar{1}0]$, and $b > \hbar\Gamma$ for $\mathbf{B} \parallel [001]$. Using the estimates $b = 1\times10^8$ eV (from the power pumped in the ultrasonic wave) and the one above, $E_{JT}/\hbar\omega_e = 1.2$, we conclude that this situation continues until the $B \approx 0.1$ T for $\mathbf{B} \parallel [110]$ or $\mathbf{B} \parallel [1\bar{1}0]$, and $B \approx 3$ mT for $\mathbf{B} \parallel [001]$. The experimental data in Fig. 1 confirms these estimates.

The system of Eqs. (15) becomes inappropriate for the description of ultrasound attenuation when $b < \hbar\Gamma^2/\Delta U$. Moreover, in the transition region $b \approx \hbar\Gamma^2/\Delta U$, there is no linear theory for ultrasound attenuation. In strong magnetic fields the energy splitting of $|x\rangle$ and $|y\rangle$ orbital states produce a new basis set of eigenstates. At $B > 0.1$ T the ultrasound wave is a small perturbation to the orbital energy levels split by the magnetic field, and the Hamiltonian of the centers interaction with the sound wave becomes nondiagonal, distinguished from that in near-zero fields in Eq. (6). This results in a resonance mechanism of attenuation caused by weak time-dependent coupling of orbital states split by the magnetic fields. Actually, it is a quasiresonance absorption, since $b \approx \hbar\omega$ and $\omega\tau_2 \ll 1$ are other conditions related to the limitations of the experiment reported in this paper for $\omega/2\pi = 33$ MHz and in Ref. [21]; it leads to very broadened resonance transitions.

Hence the increase of magnetic field induction increases the orbital splitting resulting in tail-resonance attenuation and a decrease of the attenuation curve in stronger fields. The change of regimes from relaxation to quasiresonance is supported by the experimental data in Fig. 2, where the left-hand side of the peak of attenuation remains approximately unchanged for different frequencies of the ultrasound, whereas the right-hand side of the attenuation curve (above 0.1 T) is strongly frequency dependent. Theoretical calculations of the magnetic field dependence of the attenuation in these strong magnetic fields require a more detailed analysis of the decoherence time τ_2 and its possible dependence on the magnetic field.

The total scheme of ultrasound attenuation in magnetic fields in ZnSe:Cr^{2+} is thus as follows. In zero magnetic field there is a relaxation attenuation of ultrasound driven by the relaxation time, which is determined by one-phonon processes in the absence of tunneling between equivalent Jahn-Teller configurations. In weak magnetic fields up to 0.1 T (up to 3 mT for $\mathbf{B} \parallel [001]$) the ultrasonic attenuation is still determined by the relaxation mechanism, but due to magnetic field induced tunneling there is a sharp increase in relaxation rate, which leads to a sharp increase of attenuation. Finally in magnetic fields above 0.1 T there is a transition to a quasiresonance mechanism of attenuation resulting in a smooth decrease of attenuation up to the fields of 2 T.

V. CONCLUSION

In conclusion, we revealed magnetic field induced tunneling and relaxation transitions between orthogonal distorted configurations of polyatomic systems produced by the Jahn-Teller effect of the $T\otimes e$ type in any polyatomic system. The theoretical analysis shows how the magnetic field opens a channel of relaxation via tunneling from one configuration of the system to another by coupling their otherwise orthogonal orbital states. The best conditions for experimental observation of this effect require a moderate Jahn-Teller effect with at least one vibrational state in the minima of the APES below the intersection point, but not very strong vibronic coupling that makes the tunneling too small to be significant. If the system includes spin states, the spin-orbital coupling should be much smaller than the vibronic coupling (leading to the Jahn-Teller effect). Another limitation is obvious: the magnetic field induced tunneling relaxation rate should be comparable or larger than the zero-field one. The new channel of tunneling relaxation is observed as a sharp increase in the attenuation of the ultrasound wave propagating along the [110] direction of the cubic ZnSe:Cr^{2+} crystal in relatively weak magnetic fields (<0.1 T) at low temperatures (<8 K). The effect is demonstrated for different directions of the applied magnetic field, such as [110] and [1$\bar{1}$0], and for different temperatures and frequencies. In strong magnetic fields (above 0.1 T) the relaxation attenuation mechanism is replaced by a quasiresonance mechanism, but the energy levels are greatly broadened, so only decaying tail-resonance dependence in these magnetic fields is seen. The novel effect of magnetic field induced tunneling is valid for any molecular or solid-state systems with $T\otimes e$-type vibronic coupling influencing their spectroscopic, optical, and magnetic properties, with possible applications in electronics, spintronics, and photonics.

ACKNOWLEDGMENTS

This research was carried out within the state assignment of FASO of Russia (theme "Electron" No. 01201463326), supported in part by RFBR (Projects No. 15-02-02750 and No. 16-32-00798), and by UrFU Center of Excellence Radiation and Nuclear Technologies (Competitiveness Enhancement Program). We acknowledge the support of the HLD at HZDR, a member of the European Magnetic Field Laboratory (EMFL). Also we acknowledge the support of the Government of Russia through the Program P220 Project No. 14.Z50.31.0021 (model proposed, comparison with experiment data) and RSCF Project No. 14-42-00015 (analytical calculations). One of the authors (N.S.A.) thanks the Foundation for the advancement of theoretical physics "BASIS" for support.

[1] T. Jungwirth, J. Wunderlich, V. Novak, K. Olejnik, B. L. Gallagher, R. P. Campion, K. W. Edmonds, A. W. Rushforth, A. J. Ferguson, and P. Nemec, Rev. Mod. Phys. **86**, 855 (2014).
[2] E. Y. Tsymbal, O. N. Mryasov, and P. R. LeClair, J. Phys.: Condens. Matter **15**, R109 (2003).
[3] J. R. Friedman, M. P. Sarachik, J. Tejada, and R. Ziolo, Phys. Rev. Lett. **76**, 3830 (1996).
[4] P. Politi, A. Rettori, F. Hartmann-Boutron, and J. Villain, Phys. Rev. Lett. **75**, 537 (1995).
[5] I. B. Bersuker and V. Z. Polinger, Zh. Eksp. Teor. Fiz. **66**, 2078 (1974) [JETP **39**, 1023 (1974)].
[6] I. B. Bersuker, *The Jahn-Teller Effect* (Cambridge University Press, Cambridge, 2006).
[7] *The Jahn-Teller Effect, A Bibliographic Review*, edited by I. B. Bersuker (IFI/Plenum, New York, 1984).
[8] I. B. Bersuker, Chem. Rev. **113**, 1351 (2013).
[9] V. Gudkov, in *The Jahn-Teller Effect: Fundamentals and Implications for Physics and Chemistry*, edited by H. Köppel, D. R. Yarkony, and H. Barentzen, Springer Series in Chemical Physics (Springer, Heildelberg, 2009), Vol. 97, p. 743.
[10] V. V. Gudkov, I. B. Bersuker, I. V. Zhevstovskikh, Y. V. Korostelin, and A. I. Landman, J. Phys.: Condens. Matter **23**, 115401 (2011).
[11] N. S. Averkiev, I. B. Bersuker, V. V. Gudkov, K. A. Baryshnikov, I. V. Zhevstovskikh, V. Y. Mayakin, A. M. Monakhov, M. N. Sarychev, V. E. Sedov, and V. T. Surikov, J. Appl. Phys. **116**, 103708 (2014).
[12] I. V. Zhevstovskikh, I. B. Bersuker, V. V. Gudkov, N. S. Averkiev, M. N. Sarychev, S. Zherlitsyn, S. Yasin, G. S. Shakurov, V. A. Ulanov, and V. T. Surikov, J. Appl. Phys. **119**, 225108 (2016).
[13] J. T. Vallin, G. A. Stack, S. Roberts, and A. E. Hughes, Phys. Rev. B **2**, 4313 (1970).
[14] J. T. Vallin and G. D. Watkins, Phys. Rev. B **9**, 2051 (1974).
[15] I. B. Bersuker, Zh. Eksp. Teor. Fiz. **44**, 1239 (1962) [JETP **17**, 836 (1963)].
[16] W. Low and J. T. Suss, Phys. Lett. **7**, 310 (1963).
[17] M. D. Sturge, J. T. Krause, E. M. Gyorgy, R. C. LeCraw, and F. R. Merritt, Phys. Rev. **155**, 218 (1967).
[18] M. D. Sturge, in *Solid State Physics: Advances in Research and Applications*, edited by F. Seitz, D. Turnbull, and H. Ehrenreich (Academic Press, New York, 1967), Vol. 20, pp. 92–211.
[19] Y. V. Korostelin and V. I. Koslovsky, J. Alloys Compd. **371**, 25 (2004).
[20] B. Lüthi, *Physical Acoustics in the Solid State* (Springer, Berlin, 2005).
[21] V. V. Gudkov, I. B. Bersuker, S. Yasin, S. Zherlitsyn, I. V. Zhevstovskikh, V. Y. Mayakin, M. N. Sarychev, and A. A. Suvorov, Solid State Phenom. **190**, 707 (2012).
[22] I. V. Zhevstovskikh, V. V. Gudkov, M. N. Sarychev, S. Zherlitsyn, S. Yasin, I. B. Bersuker, N. S. Averkiev, K. A. Baryshnikov, A. M. Monakhov, and Y. V. Korostelin, Appl. Magn. Reson. **47**, 685 (2016).
[23] V. V. Gudkov, A. T. Lonchakov, I. V. Zhevstovskikh, V. I. Sokolov, and V. T. Surikov, Low Temp. Phys. **35**, 76 (2009).
[24] V. Gudkov, A. Lonchakov, V. Sokolov, I. Zhevstovskikh, and N. Gruzdev, Phys. Status Solidi B **242**, R30 (2005).
[25] V. V. Gudkov, A. T. Lonchakov, V. I. Sokolov, I. V. Zhevstovskikh, and V. T. Surikov, Phys. Rev. B **77**, 155210 (2008).
[26] V. Gudkov, A. Lonchakov, V. Sokolov, and I. Zhevstovskikh, J. Korean Phys. Soc. **53**, 63 (2008).

[27] A. Abragam and B. Bleaney, *Electron Paramagnetic Resonance of Transition Ions* (Oxford University Press, Oxford, 2012).
[28] F. S. Ham, Phys. Rev. **138**, A1727 (1965).
[29] G. L. Bir and G. E. Pikus, *Symmetry and Strain-Induced Effects in Semiconductors* (Wiley, New York, 1974).
[30] S. I. Klokishner, B. S. Tsukerblat, O. S. Reu, A. V. Palii, and S. M. Ostrovsky, J. Chem. Phys. **316**, 83 (2005).
[31] B. Nigren, J. T. Vallin, and G. A. Slack, Solid State Commun. **11**, 35 (1972).
[32] G. Bevilacqua, L. Martinelli, E. E. Vogel, and O. Mualin, Phys. Rev. B **70**, 075206 (2004).
[33] All calculations were made numerically using the MATLAB package for a detailed account of all overlappings of the centers' wave functions.
[34] E. B. Osipov, N. A. Osipova, M. E. Mokina, S. N. Tsvetkova, and S. D. Kangliev, Semiconductors **41**, 897 (2007).
[35] N. S. Averkiev, Y. L. Ivanov, A. A. Krasivichev, P. V. Petrov, N. I. Sablina, and V. E. Sedov, Semiconductors **42**, 316 (2008).
[36] N. S. Averkiev, I. B. Bersuker, V. V. Gudkov, S. Zherlitsyn, S. Yasin, I. V. Zhevstovskikh, K. A. Baryshnikov, A. M. Monakhov, M. N. Sarychev, Y. V. Korostelin, and A. I. Landman, Solid State Phenom. **233**, 125 (2015).
[37] A. Abragam and M. Goldman, *Nuclear Magnetism: Order and Disorder* (Clarendon Press, Oxford, 1982).
[38] V. S. Vikhnin, Fiz. Tverd. Tela **20**, 1340 (1978) [Sov. Phys. Solid State **20**, 771 (1978)].
[39] N. S. Averkiev and L. E. Golub, Phys. Rev. B **60**, 15582 (1999).